



1 **Trace gas fluxes from tidal salt marsh soils: implications for carbon-**
2 **sulfur biogeochemistry**

3

4 Margaret Capooci¹ and Rodrigo Vargas ¹

5 ¹ Department of Plant and Soil Science

6 University of Delaware

7 152 Townsend Hall

8 531 South College Ave.

9 Newark, DE, USA 19716

10

11

12 *Correspondence to:*

13 Rodrigo Vargas

14 152 Townsend Hall

15 531 South College Ave.,

16 Newark, DE 19716

17 rvargas@udel.edu

18 Phone: 302-831-1386



19 **Abstract**

20 Tidal salt marsh soils can be a dynamic source of greenhouse gases such as carbon dioxide
21 (CO_2), methane (CH_4), and nitrous oxide (N_2O), as well as sulfur-based trace gases such as
22 carbon disulfide (CS_2) and dimethylsulfide (DMS) which play roles in global climate and
23 carbon-sulfur biogeochemistry. Due to the difficulty in measuring trace gases in coastal
24 ecosystems (e.g., flooding, salinity), our current understanding is based on snap-shot
25 instantaneous measurements (e.g., performed during daytime low tide) which complicates our
26 ability to assess the role of these ecosystems for natural climate solutions. We performed
27 continuous, automated measurements of soil trace gas fluxes throughout the growing season to
28 obtain high-temporal frequency data and to provide insights into magnitudes and temporal
29 variability across rapidly changing conditions such as tidal cycles. We found that soil CO_2 fluxes
30 did not show a consistent diel pattern, CH_4 , N_2O , and CS_2 fluxes were highly variable with
31 frequent pulse emissions ($>2,500\%$, $>10,000\%$, and $>4,500\%$ change, respectively), and DMS
32 fluxes only occurred mid-day with changes $>185,000\%$. When we compared continuous
33 measurements with discrete temporal measurements (during daytime, at low tide), discrete
34 measurements of soil CO_2 fluxes were comparable with those from continuous measurements,
35 but misrepresent the temporal variability and magnitudes of CH_4 , N_2O , DMS, and CS_2 .
36 Discrepancies between the continuous and discrete measurement data result in differences for
37 calculating the sustained global warming potential (SGWP), mainly by an overestimation of CH_4
38 fluxes when using discrete measurements. The high temporal variability of trace gas fluxes
39 complicates the accurate calculation of budgets for use in blue carbon accounting and earth
40 system models.

41



42 1. Introduction

43 Coastal vegetated ecosystems such as tidal salt marshes, mangrove forests, and seagrass
44 beds provide a wide range of ecosystem services, such as mitigating storm surge and providing
45 nursery areas for fish species (Barbier et al., 2011; Möller et al., 2014). They also store large
46 amounts of carbon at rates forty times higher than tropical rainforests (Rosentreter et al., 2018;
47 Duarte et al., 2005) and are referred to as “blue carbon” ecosystems. The importance of coastal
48 vegetated ecosystems in climate change policies has been recognized by the Paris Agreement
49 (UNFCCC, 2015). Prior to the Paris Agreement, there has been increased interest in better
50 quantifying the net balance between carbon storage and carbon release in coastal vegetated
51 ecosystems for both scientific and carbon market purposes. For example, the Verified Carbon
52 Standard developed a methodology to assess and verify the amount of carbon removed from the
53 atmosphere in tidal wetland and seagrass restoration projects for carbon market purposes
54 (Emmer et al., 2021). However, there are major knowledge gaps in assessing blue carbon in
55 coastal vegetated ecosystems. Specifically, the high spatial and temporal variability of
56 greenhouse gas (GHG) emissions, particularly for CH₄ and N₂O, in coastal vegetated ecosystems
57 complicates blue carbon offset calculations (Rosentreter et al., 2021; Capocci et al., 2019; Al-
58 Haj and Fulweiler, 2020; Murray et al., 2015). Thus, there is a need for developing measurement
59 protocols to fully quantify the contribution of multiple GHGs in blue carbon ecosystems.

60 To improve our understanding of blue carbon ecosystems in global biogeochemical
61 cycles we need to think beyond traditional GHG trace gases (i.e., CO₂, CH₄, N₂O). Tidal salt
62 marshes produce sulfur-based trace gases due to the prevalence of sulfur cycling within their
63 soils, which has implications for carbon-sulfur biogeochemistry and the global climate. While
64 coastal areas are major sources of sulfur gases (Kellogg et al., 1972), there is large



65 uncertainty in emission rates (Carroll et al., 1986; Andreae and Jaeschke, 1992). Dimethyl
66 sulfide (DMS) is one of the dominant sulfur-based gases emitted from salt marshes (Hines,
67 1996), and dimethylsulfoniopropionate (DMSP), a DMS precursor, can be produced by salt
68 marsh plant species *Spartina alterniflora*, *S. anglica*, and *S. foliosa* (Hines, 1996). DMS plays an
69 important role in linking together carbon and sulfur biogeochemistry in salt marsh soils. It can be
70 decomposed by not only sulfate-reducing bacteria, but can also act as a non-competitive
71 substrate for methylotrophic methanogenesis (Kiene, 1988; Kiene and Visscher, 1987; Oremland
72 et al., 1982) which allows methane production to occur in soils dominated by sulfate reduction
73 (Seyfferth et al., 2020). Another sulfur-based trace gas released from tidal salt marshes is carbon
74 disulfide (CS₂). CS₂ can be produced by biological processes (Brimblecombe, 2014) and is a
75 precursor to carbonyl sulfide (COS; Whelan et al., 2013). COS is the most abundant reduced
76 sulfur compound in the atmosphere and can form sulfate aerosols that affect the Earth's radiative
77 properties by reflecting sunlight, thereby having a cooling effect on the climate (Watts, 2000;
78 Taubman and Kasting, 1995). Despite sulfur-based trace gases playing a role in wetland soil
79 biogeochemistry and in global climate, there is a need to quantify coastal wetland sulfur
80 emissions and to connect those emissions to both the salt marsh sulfur cycle and to global
81 budgets (DeLaune et al., 2002; Whelan et al., 2013).

82 Historically, both soil GHGs and S-based fluxes are measured using manual survey
83 chambers, particularly during daytime low tide (e.g., De Mello et al., 1987) when soils are less
84 likely to be submerged and are accessible to researchers. Manual measurements have a number
85 of advantages, including the ability to sample over large areas over short periods of time
86 (Moseman-Valtierra et al., 2016; Simpson et al., 2019), but these measurements are labor-
87 intensive and provide limited information regarding temporal variability (Koskinen et al., 2014;



88 Savage et al., 2014; Vargas et al., 2011). On the other hand, recent advances in high temporal-
89 frequency soil efflux measurements (Capooci and Vargas, 2022; Diefenderfer et al., 2018;
90 Järveoja et al., 2018) have provided researchers with unprecedented temporal information to
91 better understand diel and tidal patterns, as well as the influence of pulse events on trace gas
92 emissions within salt marshes. While the use of automated systems is becoming more common
93 in measuring salt marsh fluxes, their use is limited by high instrumentation costs, electricity
94 requirements, and logistical challenges associated with installing these instruments in an
95 environment prone to flooding and with high humidity. As automated systems become more
96 prevalent, it provides researchers with the opportunity to evaluate data collected from manual
97 measurements, such as daily means, that have been used to inform models and budgets,
98 particularly for understudied trace gases such as N₂O, CS₂, and DMS.

99 The objective of this study is to characterize the spatial and temporal variability of trace
100 gases from soils in a tidal salt marsh. Specifically, we focus on CO₂, CH₄, N₂O, CS₂, and DMS
101 to assess the differences between measurements taken at a particular time of day (i.e., daytime
102 low tide) and measurements with high-temporal frequency (i.e., continuous measurements). Few
103 studies have measured GHG fluxes from tidal salt marshes using continuous, automated
104 measurements (Diefenderfer et al., 2018; Capooci and Vargas, 2022), and this is a pioneering
105 study that provides unprecedented information about the magnitudes and patterns of CS₂ and
106 DMS fluxes via continuous measurements. Furthermore, this study tests whether traditional
107 measurement protocols based on discrete temporal measurements provide similar information as
108 data derived from continuous measurements, including the calculation of the sustained global
109 warming potential (SGWP). Development of new technologies and incorporation of this



110 information has important implications for calculating greenhouse and trace gas budgets, as well
111 as the role salt marshes play in global biogeochemical cycles.

112

113 **2. Materials and methods**

114

115 *2.1 Study site*

116 The study was conducted at St. Jones Reserve, the brackish estuarine component of the
117 Delaware National Estuarine Research Reserve. The site is part of the Delaware Estuary and is
118 tidally connected to the Delaware Bay via the St. Jones River. St. Jones is classified as a
119 mesohaline tidal salt marsh (DNREC, 1999) and has silty clay loam soils (10% sand, 61% silt,
120 29% loam, Capooci et al 2019). The study was conducted in a section of the marsh dominated by
121 *Spartina alterniflora* (= *Sporobolus alterniflorus* (Loisel.); Peterson et al., 2014) and will be
122 referred to as SS as established in previous studies (Seyfferth et al., 2020; Capooci and Vargas,
123 2022). This area is lower in elevation relative to the rest of the marsh, is characterized by sulfur
124 reduction (Seyfferth et al., 2020), and covers ~66% of the salt marsh landscape (Vázquez-Lule
125 and Vargas, 2021).

126

127 *2.2 Experimental set-up*

128 The experiment was performed over the course of 6 campaigns to cover a full growing
129 season: greenup (G), maturity (M), senescence (S), and dormancy (D) as described by the
130 canopy phenology of the study site (Hill et al., 2021). The campaigns began during the latter half
131 of the 2020 growing season and continued into beginning of the 2021 growing season season
132 (M1 – 29 June to 2 July, M2 – 31 July to 3 Aug, S1 – 31 Aug to 3 Sept, S2 – 28 Sept to 1 Oct,



133 D1 – 13 Apr to 16 Apr, and G1 – 31 May to 3 June) due to delays related to the COVID-19
134 pandemic. We installed six PVC collars (diameter: 20 cm), placed ~1.2 meters apart, four
135 months prior to the beginning of the experiment in the year 2020. Any vegetation that grew
136 inside these collars in between campaigns was carefully removed prior to the start of the
137 measurements. These collars were used to set down six automated chambers (LICOR 8100-104,
138 Lincoln, Nebraska) to measure trace gas fluxes as described below.

139

140 *2.3 Trace gas flux measurements and QA/QC*

141 The autochambers were coupled with a closed-path infrared gas analyzer (LI-8100A,
142 LICOR, Lincoln, Nebraska) and a Fourier transform infrared spectrometer (DX4040, Gaset
143 Technologies Oy, Vantaa, Finland). The LI-8100A and the DX4040 were connected in parallel
144 since the DX4040 has its own internal pump and flow rates. Trace gas fluxes were measured
145 once per hour per chamber (i.e., all six chambers were measured within an hour). Measurements
146 were 5 minutes long and each chamber was flushed for 5 minutes total (pre-purge and post-purge
147 were both 2.5 minutes long) to help reduce the impacts of humidity on the instruments. Each
148 campaign lasted approximately 72 hours where approximately 416 measurements were recorded.

149 At the beginning of each campaign and every 24 hours after, we performed a zero
150 calibration on the DX4040 using ultra-pure 99.999% N₂ gas. It is recommended that zero
151 calibrations are performed every 24 hours and when the ambient temperature changes by 10°C,
152 so the experiment was paused for ~30 minutes during the zero calibrations each day. Gas fluxes
153 were calculated using Soil Flux Pro (v4.2.1, LICOR, Lincoln, Nebraska) and underwent
154 standardized quality assurance and quality control protocol as established in previous
155 publications (Capooci et al., 2019; Petrakis et al., 2017). Briefly, QAQC included removing all



156 values due to instrumental errors, comparing exponential and linear fits to select for the
157 measurement with the higher R^2 , removing all measurements during times where the R^2 for CO_2
158 < 0.90 , and removing all negative CO_2 fluxes.

159

160 *2.4 Ancillary measurements*

161 Meteorological (station: delsjmet-p) and water quality (station: Aspen Landing) data were
162 obtained from the National Estuarine Research Reserve's Centralized Data Management Office
163 (CDMO) and collected according to their protocol (System-wide Monitoring Program).
164 Meteorological data was collected using a CR1000 Meteorological Monitoring Station
165 (Campbell Scientific, Logan, UT, USA). Water quality data were measured using a YSI 6600
166 sonde (YSI Inc., OH, USA). Both data sets were cleaned and gap-filled following the protocol
167 established in Capooci et. al. (2022).

168 Phenological data were obtained from the PhenoCam network (site: stjones,
169 Seyednasrollah et al., 2019) as described previously (Trifunovic et al., 2020; Hill et al., 2021).
170 Briefly, a single mid-day photo (12:00:00 h) was selected for each of the days in the study period
171 and was visually inspected to remove images with obvious distortions. Since the images included
172 a variety of vegetation types, the region of interest delineated to only the area containing *S.*
173 *alterniflora*, the main species at the study site. Then the phenopix R package (Filippa et al.,
174 2020) was used to extract and calculate the greenness index, as well as delineate the phenophases
175 for the study period (Hill et al., 2021).

176

177 *2.5 Data analyses*



178 Daily averages and associated standard deviations were calculated for meteorological and
179 water quality data, except for the greenness index. Soil trace flux data were averaged into hourly
180 and daily means and standard deviations. For heat maps, average hourly and campaign-length
181 coefficients of variation were calculated.

182 We extracted measurements from the time series of the automated measurements to
183 represent information collected from discrete temporal measurements conducted during daytime
184 low tide. This approach aimed to represent a measurement protocol derived from manual (i.e.,
185 survey) measurements where most measurements are performed at daytime and low tide for
186 logistical reasons. To identify and extract these measurements, we identified when low tide
187 occurred during each day (between 9:00:00 and 17:00:00 h) of the campaigns from water level
188 data obtained from the tidal creek. All automated measurements that fell between 1 hour before
189 and 1 hour after low tide were extracted, averaged into a daily value, and classified as “discrete”
190 measurements. For example, if low tide fell at 13:00:00 h, all continuous measurements that fell
191 between 12:00:00 and 14:00:00 h were then extracted and averaged to obtain a daily mean. Daily
192 means were also calculated for all automated measurements collected during the day and will be
193 referred to as the “continuous” daily mean. Differences in the means and distributions of the
194 continuous and discrete fluxes were assessed using a t-test and a Kolmogorov-Smirnov test,
195 respectively.

196 Sustained global warming potential (SGWP) was calculated for both the campaign-long
197 and daytime low tide fluxes for CO₂, CH₄, and N₂O. SGWP accounts for sustained gas emissions
198 over time compared to the global warming potential which accounts for a pulse emission over
199 time (Neubauer and Megonigal, 2019). To calculate the SGWP, data from Day 2 and 3 of each
200 campaign was used since measurements on Day 1 and 4 did not always occur during daytime



201 low tide. Fluxes were converted into g m^{-2} and multiplied by the 20 and 100-year SGWP
202 (Neubauer and Megonigal, 2019). SGWP were compared to see whether extrapolating SGWP
203 from daily-averaged manual measurements done at low tide yielded similar values as hourly-
204 averaged from high temporal frequency measurements.

205

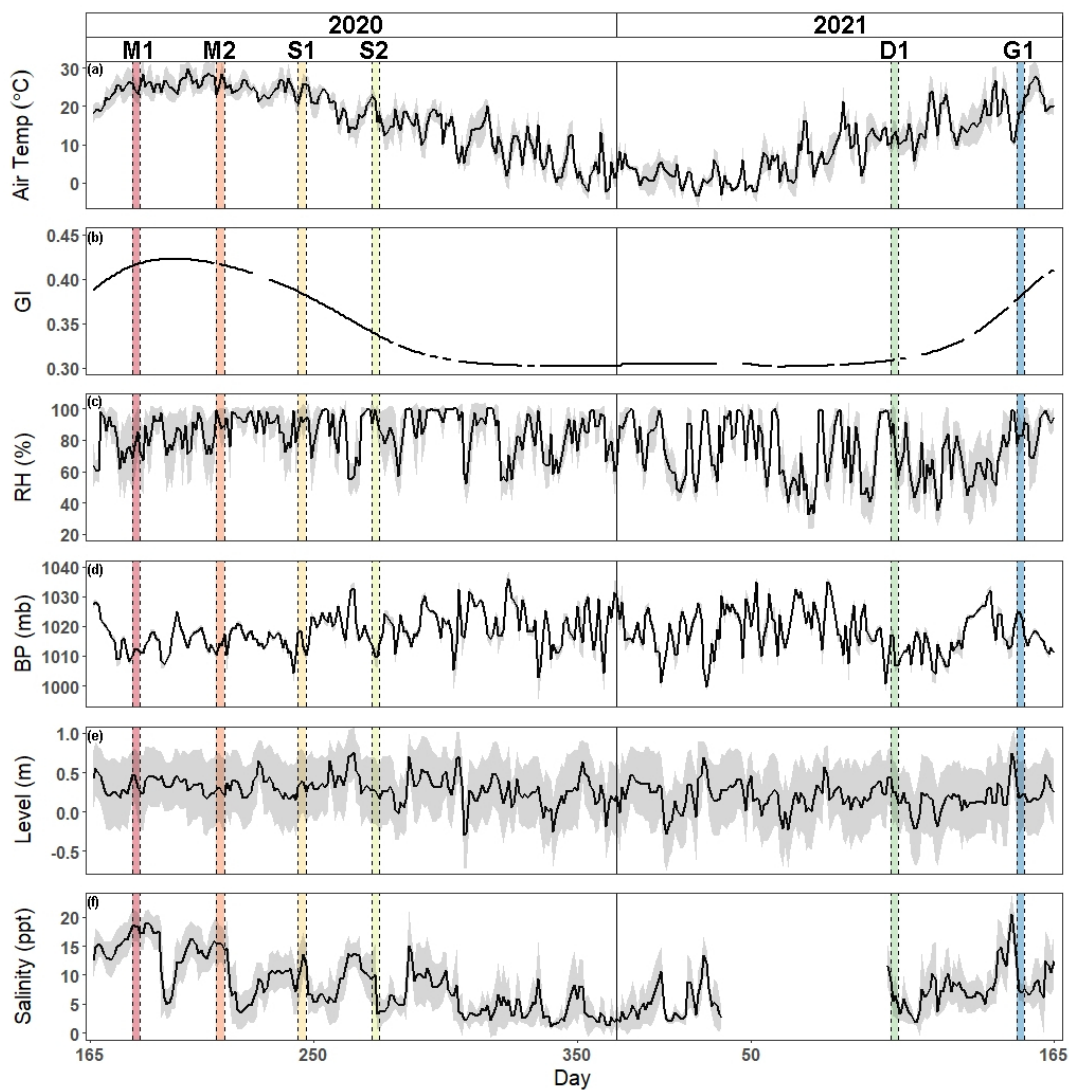
206 **3. Results**

207

208 *3.1 Meteorological and water quality*

209 Air temperature and greenness index show traditional seasonal patterns of temperate salt
210 marshes (Fig. 1). Daily mean air temperature ranged from -3.5°C to 29.9°C , with an average
211 daily temperature of $13.8 \pm 9.1^{\circ}\text{C}$, while greenness index ranged from 0.30 to 0.42 with an
212 average of 0.34 ± 0.04 . Relative humidity, barometric pressure, water level, and salinity varied
213 throughout the year. Relative humidity ranged from 32.6% to 100% with an average of $79.1\% \pm$
214 16.7% . Barometric pressure was between 999.7 and 1036 mb with an average value of $1018.3 \pm$
215 6.8 mb. Daily water level ranged from -0.30 m to 0.76 m with an average height of 0.25 ± 0.2 m,
216 while salinity ranged from 1.1 ppt to 20.4 ppt with an average of 8.0 ± 4.45 ppt.

217



218

219 **Figure 1.** Time series of hourly mean \pm SD (gray shaded region of (a) air temperature, (b)
220 greenness index, (c) relative humidity, (d) barometric pressure, (e) water level, and (f) salinity
221 from June 14, 2020 to June 14, 2021. Vertical shaded areas correspond to each of the campaigns
222 (M = maturity, S = senescence, D = dormancy, G = greenup).

223

224



225 *3.2 Greenhouse gas and sulfur-based trace gas patterns and variability*

226 Average CO₂ fluxes were significantly different in each campaign, with the highest
227 average fluxes occurring during the G1 campaign and the lowest during the D1 campaign (Fig.
228 2a). During some campaigns, such as S1, CO₂ fluxes did not show similar temporal patterns
229 between chambers, whereas during other campaigns, such as M2 and G1, all six chambers had
230 similar patterns. While there is a seasonal pattern in CO₂ fluxes, with higher fluxes occurring
231 during warmer months, diel patterns were not consistent between campaigns. One notable
232 exception is the G1 campaign, during which a clear diel pattern was observed. CO₂ fluxes had
233 consistent variability from one hour to the next during each of the 6 campaigns (Fig. 3a), with
234 overall average variability ranging from 28.9% during M2 to 49.6% during D1.

235 CH₄ fluxes were low most of the time, particularly during the G1 campaign (Fig. 2b).
236 However, CH₄ pulses occurred during 5 out of the 6 campaigns, with S1 and S2 having the most
237 frequent pulse emissions. S2 had the largest CH₄ pulse, 13,488 nmol m⁻² s⁻¹, which was 2,599%
238 higher than the average flux. The highest average CH₄ fluxes also occurred during S1 and S2,
239 while the highest hourly variability occurred in both S1 and S2, as well as in M2 (Fig. 3b). Mean
240 CH₄ variability ranged from -108% in M1 to 91.0% in S1.

241 Most N₂O fluxes were near-zero, with periodic pulses of emissions or uptake that ranged
242 from -33.8 to 19.0 nmol m⁻² s⁻¹ (Fig. 2c), with a maximum percent change from the mean of
243 10,231%. Four out of the six campaigns (M1, S2, D1, and G1) had net N₂O uptake, while two
244 campaigns (M2, S1) had net N₂O fluxes. There were no significant differences between
245 campaigns except for M1 and S1. Meanwhile, N₂O fluxes had very high hourly variability
246 ranging from -106,964% to 26,208% (Fig. 3c). Consequently, average variability during each
247 campaign was highly variable from -1,032% to 129%.



248 Similarly to CH₄ and N₂O, CS₂ fluxes were low the majority of the time, with occasional
249 pulses of emissions or uptake (Fig. 2d). CS₂ fluxes ranged from -386.9 to 306.2 nmol m⁻² s⁻¹,
250 with a maximum percent change from the mean of 4,785%. All campaigns had net emissions
251 despite periodic pulses of CS₂ uptake. CS₂ fluxes also had high hourly variability, with overall
252 means for each campaign ranging from -70.2% during D1 to 2254% during M2 (Fig. 3d).

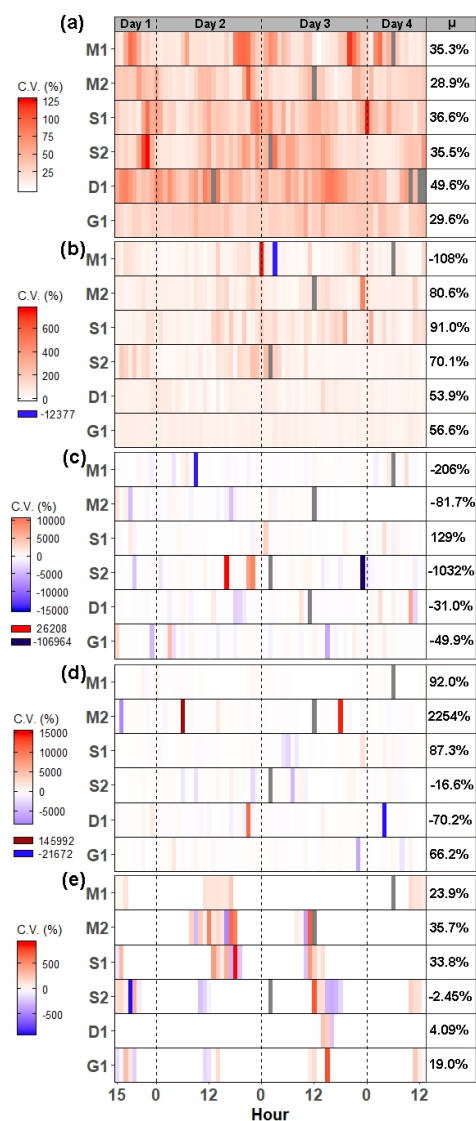
253 DMS emissions were zero for most of the campaigns (Fig. 2e). Pulses of emissions and
254 uptake tended to occur during mid-day. DMS fluxes ranged from -158.5 to 230 nmol m⁻² s⁻¹,
255 with a maximum percent change from the mean of 185,987%. D1 and G1 had net uptake, while
256 the other four campaigns had net emissions of DMS. During periods of emissions and uptake,
257 hourly variability ranged from -870.5% to 888.7% (Fig. 2e). The extended periods of no DMS
258 fluxes contributed to low overall mean variability during each campaign, ranging from -2.45% in
259 S2 to 35.7% in M2.

260



261

262 **Figure 2.** Time series of fluxes from each chamber during each campaign for (a) CO₂, (b) CH₄,
263 (c) N₂O, (d) CS₂, and (e) DMS. Each color designates a different chamber. The campaign means
264 [LCI, UCI] are listed on each panel. The y-axis for CH₄ fluxes was shortened to show the
265 variability. Full range of CH₄ fluxes during S2 can be seen in Supplementary Figure (SF) 1.



266

267 **Figure 3.** Heat maps of hourly coefficient of variance (CV) for (a) CO₂, (b) CH₄, (c) N₂O, (d)
 268 CS₂, and (e) DMS during each campaign. Each pixel represents the average CV for that hour.
 269 Mean CV for each campaign is listed in the μ column. Grayed out pixels represent NA. Note:
 270 legend scale is different for each gas and campaigns start at 15:00:00 h on Day 1 and end at
 271 13:00:00 h on Day 4.



272 *3.3 Comparisons between continuous and discrete measurement scenarios*

273 A subset of the continuous measurements that fall during daytime low tide was selected
274 to represent data collected using traditional discrete, manual measurements which are commonly
275 reported for tidal salt marshes. Information from continuous and discrete datasets are compared
276 to evaluate whether they provide similar distributions, daily means, flux-temperature
277 relationships, and SGWP.

278 Continuous and discrete flux distributions can be seen via density plots (Fig. 4). While
279 the distributions for continuous and discrete fluxes overlap for each of the five gases, four of the
280 five gases have significantly different distributions of fluxes when comparing the continuous and
281 the discrete datasets (Table 1). The only gas that had similar distributions between the two
282 sampling intervals was CO₂ (Table 1). For all gases, the continuous distribution had higher
283 kurtosis values and higher C.V. than the discrete fluxes (Table 1). Of the five gases, CS₂ was the
284 only one with a more skewed discrete data distribution and significantly different means between
285 continuous and discrete measurement scenarios (Fig. 4b, Table 1).

286 For CS₂ and DMS, discrete measurements had higher overall daily mean fluxes (Fig. 5d,
287 5e), while the opposite occurred for CH₄ and N₂O (Fig. 5b, 5c). CO₂ fluxes from continuous and
288 discrete measurements had nearly a 1:1 relationship (Fig. 5a). Both CO₂ and DMS had strong
289 relationships between continuous and discrete daily means, with r-squares higher than 0.7, while
290 N₂O and CS₂ had moderate relationships. CH₄ had a poor fit between continuous and discrete
291 measurements.

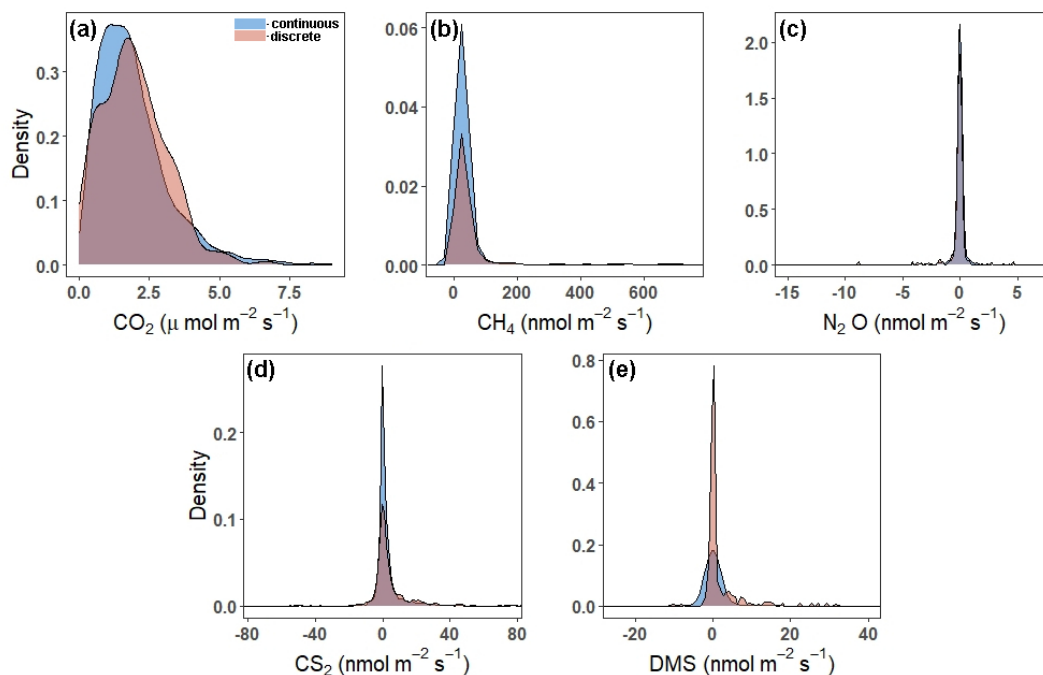
292 Next, relationships between trace gas flux and air temperature were evaluated for each
293 gas under continuous and discrete measurement scenarios. CO₂ and CH₄ fluxes had statistically
294 significant relationships for both discrete and continuous measurements versus air temperature



295 (Fig. 6a-d). Air temperature explained 38% and 21% of the variability for discrete and
296 continuous measurements for CO₂, respectively (Fig. 6a, b), while air temperature explained
297 32% and 7% of the variability for discrete and continuous measurement for CH₄ (Figs. 6c, d).
298 The slopes for both discrete and continuous CO₂ fluxes were not significantly different (95% CI;
299 0.029 - 0.12, 0.037 - 0.054, respectively), as well as for CH₄ (95% CI; 2.14 - 12.7, 1.31 - 2.71,
300 respectively). For N₂O, CS₂, and DMS, there were no significant relationships between discrete
301 daily mean fluxes and air temperature, but there were significant relationships between
302 continuous hourly mean fluxes and air temperature (Fig. 6e-j). Air temperature explained very
303 little variability for N₂O, CS₂, and DMS.

304 Discrete measurements had a higher SGWP potential than the continuous measurements.
305 While the discrete measurements had a slightly lower SGWP for CO₂ and a slightly higher
306 SWGP for N₂O, the difference between continuous and discrete SGWP was driven by CH₄. The
307 20-yr and 100-yr SGWP for discrete measurements of CH₄ were up to ~38% higher than the
308 respective continuous measurements, contributing to an overall increase of ~18% and ~11% for
309 the discrete measurement's 20- and 100-year SGWP.

310



311

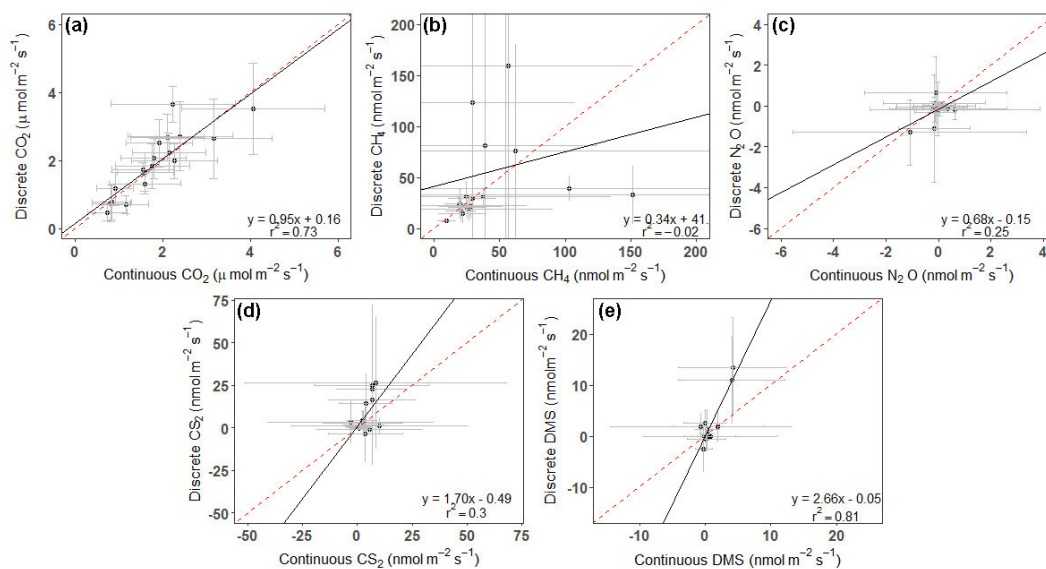
312 **Figure 4.** Density plots comparing the distribution of fluxes throughout all campaigns
313 (continuous) to those measured during daytime low tide (discrete) for (a) CO₂, (b) CH₄, (c) N₂O,
314 (d) CS₂, and (e) DMS. Note: The scales on the x- and y-axes are different. The tails have been
315 cut off to better see the peaks for (b), (c), (d), and (e). To see plots with full distributions, see SF
316 2.



317 **Table 1.** Summary of continuous and discrete measurement data and distributions for each gas.
 318 An alpha of < 0.05 was used to determine significant differences between the means and the
 319 distributions. Note: Means for CO_2 are in $\mu\text{mol m}^{-2} \text{s}^{-1}$, while the other gases are in $\text{nmol m}^{-2} \text{s}^{-1}$.
 320

Gas	Sampling Frequency	Mean	95% CI	C.V.	Skewness	Kurtosis	Means Different?	Distributions Different?
CO_2	Continuous	1.92	1.86–1.97	67.2%	1.53	6.51		
	Discrete	1.90	1.74–2.07	62.3%	0.67	3.65	No	No
CH_4	Continuous	41.2	29.5–52.9	708%	41.6	1903		
	Discrete	57.6	39.2–76.0	234%	5.21	34	No	Yes $p = 0.02$
N_2O	Continuous	-0.06	-0.13–0.009	2686%	-4.67	133		
	Discrete	-0.16	-0.29–0.04	556%	-4.39	47.8	No	Yes $p < 0.001$
CS_2	Continuous	3.39	2.45–4.33	673%	1.51	116		
	Discrete	6.44	3.70–9.18	312%	3.93	22.9	Yes $p = 0.04$	Yes $p = 0.05$
DMS	Continuous	1.11	0.70–1.51	907%	8.74	223		
	Discrete	1.77	1.06–2.48	295%	3.40	16.6	No	Yes $p < 0.001$

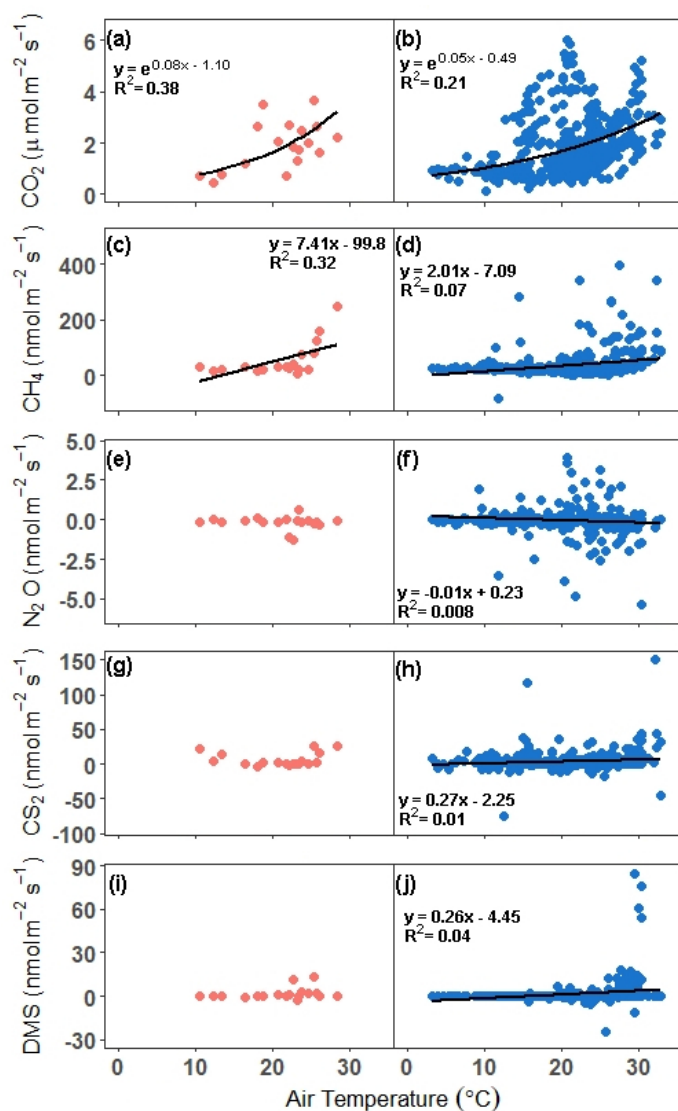
321



322

323

324 **Figure 5.** Plots comparing the daily average of continuous to discrete measurements for (a) CO_2 ,
325 (b) CH_4 , (c) N_2O , (d) CS_2 , and (e) DMS. Error bars represent the SD and have been cut off in
326 panel (b) to show data better. See SF 3 for full error bars for panel b. Red dashed line is the 1:1
327 line, while the black solid line is the trend line.



328

329 **Figure 6.** Comparison of fluxes versus air temperature for all campaigns. In panels, a, c, e, g, and
330 I, the hourly continuous mean is compared to the hourly air temperature, while in panels b, d, f,
331 h, and k, the discrete daily mean is compared to the daily air temperature. The trend lines for
332 significant relationships at $\alpha < 0.05$ are plotted. Note: In panel d, the outlier hourly mean of
333 2,275 $\text{nmol m}^{-2} \text{s}^{-1}$ is not included in the trend line or in the graph.



334 **Table 2.** Sustained global warming potential (SGWP) derived from continuous and discrete
335 temporal (during daytime low tide) measurements in a tidal salt marsh.

336

Frequency	CO ₂ (g m ⁻²)	CH ₄ (CO ₂ -eq (g m ⁻²))		N ₂ O (CO ₂ -eq (g m ⁻²))		Total (CO ₂ -eq (g m ⁻²))	
		20-yr SGWP	100-yr SGWP	20-yr SGWP	100-yr SGWP	20-yr SGWP	100-yr SGWP
Continuous	84.9	70.4	33.0	0.27	0.30	155.57	118.2
Discrete	82.7	103.2	48.4	0.40	0.44	186.3	131.54

337

338

339 4. Discussion

340 4.1 Measuring all the time: seasonal and diel patterns and hot moments of soil trace gases

341 Spatial variability between the individual chambers at SS were low, but CO₂ fluxes
342 showed temporal variability that corresponded to changes in temperature. The relatively low
343 spatial variability within our experimental setting contrasts with previously reported high spatial
344 variability of CO₂ fluxes attributed to the presence of a hot spot (Capooci and Vargas, 2022).
345 However, previous CO₂ fluxes measured at the SS site ranged from 0-10 μmol m⁻² s⁻¹, with the
346 bulk of the measurements between 0-4 μmol m⁻² s⁻¹, with higher fluxes associated with hot spots
347 or warmer temperatures (Capooci and Vargas, 2022; Seyfferth et al., 2020). Therefore, location
348 of measurements within a landscape could be influenced by hot spots, which complicates
349 ecosystem scale calculations of soil CO₂ fluxes (Barba et al., 2018). In addition, there was a
350 seasonal pattern evident in the CO₂ fluxes, with higher emissions during the growing season, as
351 typical in temperate ecosystems, as well in the significant relationship between CO₂ and air
352 temperature. Other studies at temperate wetland sites have found higher fluxes during the



353 summer (Simpson et al., 2019; Yu et al., 2019; Bridgham and Richardson, 1992), as well as
354 relationships between CO₂ fluxes and temperature (Capooci and Vargas, 2022; Simpson et al.,
355 2019; Xie et al., 2014) highlighting that CO₂ fluxes in temperate salt marshes exhibit a
356 temperature dependency over seasonal scales, even in the presence of tides.

357 While CO₂ fluxes show seasonal patterns, there are no diel patterns that persist
358 throughout the year. During G1, the peak of high tide coincided with peak daily temperature.
359 This scenario also occurred during D1, but fluxes were too low to discern patterns. During all
360 other campaigns, low tide and peak temperatures coincided. These results suggest that diel
361 patterns may occur periodically under certain conditions. For example, at the SS site, it may be
362 that diel patterns occur during high tide at the temperature peak. While we expected the highest
363 fluxes during low tides due to increased oxygen exposure, there may be a lag between low tide in
364 the creek and low water levels at the SS site, resulting in higher fluxes during high tide in the
365 creek. However, these results can vary from site to site and with proximity to the tidal creek.
366 More research using high temporal frequency measurements are needed to parse out the role of
367 temperature and tides on CO₂ fluxes across salt marshes to properly represent the pattern in earth
368 system models (Ward et al., 2020)

369 Similarly to CO₂, CH₄ has a significant relationship with air temperature, however it
370 explains less variability in the fluxes. Several studies have found positive correlations between
371 soil CH₄ fluxes and temperature (Bartlett et al., 1985; Emery and Fulweiler, 2014; Wang and
372 Wang, 2017) in temperate salt marshes, while others have not (Wilson et al., 2015). It is
373 important to note that while, in general, salt marsh CH₄ fluxes are positively related to
374 temperature (Al-Haj and Fulweiler, 2020), the ability of temperature to explain CH₄ flux
375 variability is low, compounded by many, often site-specific, factors that affect methane



376 production and consumption, such as organic matter supply, microbial communities, and
377 diffusion rates (Al-Haj and Fulweiler, 2020; Bartlett et al., 1985).

378 At our study site, CH₄ fluxes were highest and pulses were most frequent during
379 senescence, agreeing with findings from ecosystem-scale measurements derived using the eddy
380 covariance technique (Vázquez-Lule and Vargas, 2021). In most wetland ecosystems, the highest
381 fluxes have been reported during the summer (Kim et al., 1998; Rinne et al., 2007; Van Der Nat
382 and Middelburg, 2000; Livesley and Andrusiak, 2012), but we highlight that there is a lack of
383 measurements during the winter (Al-Haj and Fulweiler, 2020). In *S. alterniflora* marshes, highest
384 mean CH₄ fluxes have been found in both the summer and the fall (Bartlett et al., 1985; Emery
385 and Fulweiler, 2014). At a site dominated by *S. alterniflora*, both high fluxes and porewater CH₄
386 concentrations were found in September, indicating either a continual build-up of CH₄ in the
387 pore water over the growing season and/or increased CH₄ production in the fall. For our site, it is
388 likely higher CH₄ emissions during senescence were due to an input of labile organic matter
389 from plant die-off (Seyfferth et al., 2020). Furthermore, a recent study has shown that porewater
390 DMS, a non-competitive substrate for methylotrophic methanogenesis that is produced from the
391 breakdown of DMSP, a metabolite produced by *S. alterniflora* (Dacey et al., 1987), peaks during
392 the fall (Tong et al., 2018). Therefore, we postulate that an influx of DMS may also contribute to
393 higher CH₄ fluxes during senescence in marshes dominated by *S. alterniflora*. This finding
394 highlights the importance of carbon-sulfur biogeochemistry and measuring fluxes during non-
395 summer months; particularly in marshes that have plant communities that provide substrates used
396 in methylotrophic methanogenesis (Seyfferth et al., 2020).

397 On a diel timescale, pulse emissions of CH₄ from the soil tend to occur during the
398 warmest time of the day, as well as during low and rising tides. There are very few studies that



399 report high-temporal frequency data of CH₄ emissions, most of which include plants within their
400 scope (via transparent chambers or eddy covariance) or focus on tidal creeks, making it difficult
401 to ascertain whether the diel patterns seen in this study are typical of tidal salt marsh soils.
402 Considering the broader range of studies about CH₄ fluxes in coastal vegetated ecosystems, CH₄
403 emissions have been found to peak at various points in the day, from during the day (Yang et al.,
404 2018, 2017; Tong et al., 2013), at night (Diefenderfer et al., 2018), or highly variable (Jha et al.,
405 2014; Xu et al., 2017). At our site, CH₄ fluxes tended to peak at the confluence of peak daily
406 temperature and low to rising tides, indicating that physical forcing may contribute to CH₄ pulses
407 (Bahlmann et al., 2015; Middelburg et al., 1996). However, pulses did occur during other times
408 throughout the day and within the tidal cycle. While some of the pulse emissions may be a result
409 of ebullition, the majority are associated with high R²'s, indicating that they are sustained over
410 the measurement period. Our results demonstrate the importance of conducting high-temporal
411 frequency CH₄ measurements in tidal salt marsh soils for several reasons, including the need for
412 more data to better understand the drivers of CH₄ fluxes at diel scales and how that affects model
413 predictions.

414 N₂O emissions and uptake loosely followed a seasonal pattern, likely driven by the
415 canopy phenological stages. During the growing season, it has been shown that highly
416 productive plants can compete with soil microbes for NO₃⁻ and NH₄⁻ (Cheng et al., 2007; Yu et
417 al., 2012; Zhang et al., 2013; Granville et al., 2021; Xu et al., 2017), shifting denitrifiers into
418 consuming N₂O and resulting in a net uptake during G1 and M1. As the plants reach peak
419 maturity, the system shifts into net emission of N₂O during M2 and S1. One study found that
420 nitrogen additions resulted in a pulse of N₂O in July when most of the plant growth had occurred,
421 but no response in April, suggesting that the competition for NO₃⁻ and NH₃⁺ decreases when



422 plant growth has slowed down (Moseman-Valtierra et al., 2011). Increased substrate availability
423 combined with warm temperatures likely contributed to the marsh being a net source of N₂O
424 during the later stages of the growing season. As temperatures drop, the system shifts back into
425 net uptake, as seen during S2 and D1. Similar seasonal patterns have been seen in other studies,
426 albeit shifted by a month or two depending on the local climate and phenophases (Granville et
427 al., 2021; Emery and Fulweiler, 2014). These findings highlight balance between processes that
428 produce N₂O (e.g., nitrification, denitrification, and nitrifier-denitrification) and consume N₂O
429 (e.g., denitrification), as well as substrate availability and plant phenology in determining
430 whether a marsh is a source or sink of N₂O at any given point.

431 As with seasonality, diel patterns of N₂O showed both emissions and uptake. Several
432 studies have also reported both emissions and uptake during a 24-hour period (Yang et al., 2017;
433 Tong et al., 2013). We found that pulses of uptake and emissions occurred both during the day
434 and at night, as well as during different phases of the tidal cycle. Studies have found higher
435 fluxes during the day (Tong et al., 2013; Yang et al., 2017) and at night (Laursen and Seitzinger,
436 2002; Yang et al., 2017; Bauza et al., 2002). Generally, fluxes were slightly higher at night
437 throughout the campaigns, perhaps as a result of increased availability of NH₄⁺ at night due
438 decreased competition from photosynthesizers (Bauza et al., 2002). Overall, N₂O fluxes were
439 near-zero with a < 0.50 nmol m⁻² s⁻¹ difference between daytime and nighttime mean fluxes,
440 suggesting that N₂O fluxes do not play a major role in GHG emissions at this salt marsh.

441 Our automated measurements of sulfur-based trace gases show high variability in CS₂,
442 with low fluxes punctuated by occasional pulse emissions. There are no previous studies with
443 automated measurements to compare our findings, but previous studies have noted that CS₂
444 fluxes are highly variable (Stuedler and Peterson, 1985; Hines, 1996), with periods of emission



445 and uptake. However, fluxes at SS were, on average, an order of magnitude higher than values
446 reported in the literature (Supplementary Table 1). There could be several reasons for the
447 difference in magnitudes: 1) improvement in instrumentation to detect CS₂, 2.) sampling
448 technique differences, and 3.) site-specific characteristics. Since the influx of sulfur-based trace
449 gas measurements in the 1980s, instrumentation has advanced from using molecular sieves and
450 cryotrap to store samples before measuring them on a gas chromatograph (e.g., Carroll et al.,
451 1986; Cooper et al., 1987; Steudler and Peterson, 1984) to using portable Fourier transform
452 infrared (FTIR) spectrometers that measure trace gas concentrations in near real-time. These
453 instrumentation advances subsequently led to changes in sampling techniques. Traditionally, it
454 was common to keep the chamber closed for upwards of 24-hours, with samples being collected
455 over hourly intervals throughout the day (Carroll et al., 1986; Goldan et al., 1987). Sweep air
456 free of sulfur trace gases was also commonly used to avoid the need to take samples at both the
457 inlet and outlets of the chambers (Goldan et al., 1987). However, others used ambient air because
458 it more closely resembled *in situ* conditions (Steudler and Peterson, 1985). With recent advances,
459 sampling techniques have changed to eliminate the need for very long closure times and reduce
460 the effects the chambers have on micrometeorological conditions. Now, high-temporal
461 frequency, long-term data can be obtained, thereby capturing pulse emissions that otherwise may
462 be missed. The third reason for difference in magnitude could be due to site-specific differences
463 in CS₂ fluxes. While the mechanisms by which CS₂ is produced are poorly understood, there are
464 several potential production pathways: OM degradation, photochemical production, and algal
465 production (Xie and Moore, 1999). The most likely pathway for our site is the microbially-
466 mediated reaction between H₂S and organic matter due to high sulfur concentrations, anaerobic
467 conditions, and a large pool of decaying organic matter. Finally, CS₂ is a short-lived sulfur gas



468 but the major product of CS₂ oxidation is COS; consequently, understanding CS₂ production and
469 oxidation is important for recognizing the role of salt marshes in COS dynamics (Whelan et al.,
470 2013).

471 The mean of measured DMS fluxes generally fall within those reported in the literature,
472 but with pulses higher than previously reported and different temporal patterns. We found that
473 DMS fluxes only occurred during the middle of the day, near when air temperatures peaked. This
474 is contrary to several studies that have found DMS fluxes during other times of the day
475 (Morrison and Hines, 1990; Steudler and Peterson, 1985; DeLaune et al., 2002). Some studies
476 have found diel patterns related to temperature (De Mello et al., 1987; Cooper et al., 1987b) and
477 incoming tides (Morrison and Hines, 1990; Dacey et al., 1987; Goldan et al., 1987). Our results
478 indicate that DMS fluxes from the SS site are associated with temperature and light-related
479 processes, whether these variables influence microbial activity, plant physiology, or a
480 combination of both. A study found that DMS fluxes peaked after a full daylight period in a
481 Danish estuary (Jørgensen and Okholm-Hansen, 1985). However, there is no information on the
482 diel patterns of DMS in the sediment pore water or its release from *S. alterniflora* plants. DMS is
483 also produced by other pathways that occur under anoxic conditions, such as methylation of
484 sulfide and methanethiol (Lomans et al., 2002; Sela-Adler et al., 2015), microbial reduction of
485 dimethylsulfoxide (Capone and Kiene, 1988), and/or the incorporation of inorganic substrates
486 (i.e., CO₂) and organic methylated compounds (Finster et al., 1990; Moran et al., 2008; Lin et al.,
487 2010). To better understand DMS fluxes, more research into the dynamics between *S.*
488 *alterniflora*, pore water DMS, and DMS fluxes is needed, as it plays an important role in carbon-
489 sulfur biogeochemistry, particularly as a non-competitive substrate for methylotrophic
490 methanogenesis (Seyfferth et al., 2020).



491

492 *4.2 Continuous versus discrete measurements: do we get the same information?*

493 Our results show that discrete temporal measurements of CO₂ during daytime low tide
494 throughout the year (including dormancy) may be sufficient to obtain a representative mean of
495 the temporal variability of soil CO₂ flux. This has implications for calculating carbon budgets.
496 Furthermore, the distribution of continuous and discrete CO₂ fluxes is similar, indicating that
497 discrete measurements are capturing similar variability as continuous measurements. This
498 observation is reinforced by the CO₂ ~ air temperature relationships, which do not have
499 significantly different slopes (discrete: 0.03 - 0.12, continuous: 0.04 - 0.05), providing further
500 support for the utility of daytime low tide discrete measurements in evaluating potential drivers
501 of CO₂ variability.

502 In contrast, high variability in CH₄ fluxes resulted in the means for discrete and
503 continuous measurements to be similar, but with significantly different distributions. In salt
504 marshes, CH₄ fluxes are characterized by high variability (Rosentreter et al., 2021), making it
505 difficult to assess the processes that control CH₄ fluxes (Vázquez-Lule and Vargas, 2021). While
506 the means were not significantly different despite ~33% higher mean flux using discrete
507 measurements, it is important to note that the 95% confidence interval and the coefficient of
508 variation are broad and very high, resulting in potential error cancellation for the calculation of
509 the mean. We postulate that the discrete measurement approach can be used to calculate budgets
510 with the caveat of large uncertainties and that they likely overestimate the mean CH₄ flux.
511 Discrete measurements do not capture similar variability as the continuous measurements and
512 have a stronger air temperature-CH₄ flux relationship than continuous measurements, despite the
513 overlap between their confidence intervals (2.14 - 12.7 and 1.31 - 2.71, respectively). However,



514 continuous measurements provide a more accurate depiction of the patterns and magnitudes of
515 CH₄ and can provide stronger insights into the interrelated drivers of CH₄ fluxes.

516 Regardless of the sampling interval, N₂O fluxes had means that are near-zero. Due to
517 fluxes consistently being near zero, the discrete and continuous measurements will likely get
518 similar overall results due to error cancellation even if the distributions were significantly
519 different. The continuous measurements capture a wider range of fluxes than the discrete
520 measurements, as seen with its very high coefficient of variance and a different distribution.
521 However, the skewness between the two approaches is very similar, due to the bulk of the
522 measurements falling around the same values. It is important to note that this site is nitrogen-
523 limited, which constrains N₂O production. In marshes that are not nitrogen-limited, sampling
524 intervals will likely play a more important role since fluxes will be higher.

525 For CS₂, discrete and continuous measurements did not have similar means or
526 distributions, likely due to the high variability found in these measurements. Previous studies
527 using discrete measurements of CS₂ have noted its high variability (e.g. De Mello et al., 1987),
528 with one highlighting the need for frequent measurements of sulfur-based trace gases during the
529 day in order to obtain an accurate mean daily flux value (Stuedler and Peterson, 1985). We found
530 that discrete measurements taken during daytime low tide result in a daily mean that is nearly
531 twice that of the daily mean from the continuous measurements. The average CS₂ fluxes
532 measured during our field campaigns were up to an order of magnitude higher than previously
533 reported. We advocate for more measurements of CS₂ fluxes beyond focusing on low tide
534 windows and during different canopy phenological phases across salt marshes to better
535 understand the dynamics of this trace gas.



536 When measuring DMS fluxes during daytime low tide, the mean is similar to the
537 continuous measurement mean, but the distributions are significantly different. However, caution
538 should be taken in using discrete measurements of DMS to calculate daily means, particularly if
539 those measurements fall during the warmest part of the day when DMS fluxes are the most
540 active. This could result in overestimating the daily mean since extended periods of no fluxes are
541 not accounted for. One approach to measuring DMS fluxes would be to use the strong
542 relationship between discrete and continuous measurements to correct for the overestimation of
543 discrete fluxes. However, this approach would still require the use of a continuous, automated
544 system at different points throughout the year to establish a site-specific correction of discrete
545 mean DMS fluxes, particularly if DMS fluxes are used to calculate DMS budgets.

546

547 **5. Conclusion: what are we missing: potential caveats?**

548 Discrete measurements have the clear advantage of capturing the spatial variability of soil
549 trace gas fluxes across an ecosystem, but this approach is also used to describe the temporal
550 variability. Here we discuss the advantages and differences from discrete and continuous
551 measurements derived from this study. Discrete measurement campaigns are suitable for
552 calculating budgets, particularly for CO₂ and N₂O since they capture very similar means. While
553 we found that CH₄ and DMS means were not significantly different between the two approaches,
554 there are caveats that must be considered when using discrete measurements. The high variability
555 inherent in CH₄ fluxes can contribute to the lack of significant differences between the two
556 approaches and result in discrete measurements overestimating the overall CH₄ fluxes from a
557 tidal salt marsh. This has implications when calculating SWGP where differences in CH₄ means
558 largely contribute to the differences in SGWP between the two approaches and can affect how



559 scientists and policymakers view tidal salt marshes and blue carbon as a natural climate solution
560 (Macreadie et al., 2021). For DMS, it is important to assess diel patterns to ensure that fluxes are
561 representative, particularly at sites that have patterns similar to what is seen at our study site.
562 When evaluating variability or trying to parse out the processes that drive GHG and trace gas
563 emissions from tidal salt marshes, using continuous, automated measurements would be the best
564 approach. This is particularly important for CH₄, where pulse emissions are frequent during the
565 growing season and can be very high. Using continuous measurements is also important in
566 scenarios where discrete measurements do not capture a similar mean or distribution, as with CS₂
567 fluxes. However, discrete measurements are more capable of representing spatial variability, and
568 until we have a better understanding of which source of variability is higher, temporal, or spatial,
569 both techniques should be considered for ecosystem assessments.

570

571 **Data availability**

572 Meteorological (station: delsjmet-p) and water quality (station: Aspen Landing) data are
573 available from the National Estuarine Research Reserve's Centralized Data Management Office
574 (CDMO) at <https://cdmo.baruch.sc.edu/>. Phenological data are available from the PhenoCam
575 network (site: stjones) at <https://phenocam.sr.unh.edu/webcam/sites/stjones/>. Data from trace gas
576 fluxes will be publicly available in a FAIR data repository (e.g., Figshare) before publication of
577 this research.

578

579 **Author contributions**

580 MC and RV conceptualized the study, designed the methodology, and conducted project
581 administration. MC conducted the formal analysis, investigation, and visualization, as well as



582 wrote the original draft. RV provide funding, resources, supervision, as well as reviewed and
583 edited the manuscript.

584

585 **Competing interests**

586 The authors declare that they have no conflict of interest.

587

588

589 **Acknowledgments**

590 This research was supported by the National Science Foundation (#1652594). MC acknowledges
591 support from an NSF Graduate Research Fellowship (#1247394). We thank the onsite support
592 from Kari St. Laurent and the Delaware National Estuarine Research Reserve (DNERR), as well
593 as from Victor and Evelyn Capooci for field assistance during the first campaign. We thank
594 George Luther for inspiring discussions about carbon-sulfur biogeochemistry in salt marshes.
595 The authors acknowledge the land on which they conducted this study is the traditional home of
596 the Lenni-Lenape tribal nation (Delaware nation).



597 **References**

- 598 Al-Haj, A. N. and Fulweiler, R. W.: A synthesis of methane emissions from shallow vegetated
599 coastal ecosystems, *Glob. Chang. Biol.*, 26, 2988–3005, <https://doi.org/10.1111/gcb.15046>,
600 2020.
- 601 Andreae, M. O. and Jaeschke, W. A.: Exchange of sulfur between biosphere and atmosphere
602 over temperate and tropical regions, in: *Sulfur Cycling on the Continents*, edited by:
603 Howarth, R. W., Stewart, J. W. B., and Ivanov, M. V., Wiley, New York, 1992.
- 604 Bahlmann, E., Weinberg, I., Lavrič, J. V, Eckhardt, T., Michaelis, W., Santos, R., and Seifert, R.:
605 Tidal controls on trace gas dynamics in a seagrass meadow of the Ria Formosa lagoon
606 (southern Portugal), 12, 1683–1696, <https://doi.org/10.5194/bg-12-1683-2015>, 2015.
- 607 Barba, J., Cueva, A., Bahn, M., Barron-Gafford, G. A., Bond-Lamberty, B., Hanson, P. J.,
608 Jaimes, A., Kulmala, L., Pumpanen, J., Scott, R. L., Wohlfahrt, G., and Vargas, R.:
609 Comparing ecosystem and soil respiration: review and key challenges of tower-based and
610 soil measurements, *Agric. For. Meteorol.*, 249, 434–443,
611 <https://doi.org/10.1016/j.agrformet.2017.10.028>, 2018.
- 612 Barbier, E., Hacker, S., Kennedy, C., Stier, A., and Silliman, B.: The value of estuarine and
613 coastal ecosystem services, *Ecol. Monogr.*, 81, 169–193, 2011.
- 614 Bartlett, K. B., Harriss, R. C., and Sebacher, D. I.: Methane flux from coastal salt marshes, *J.*
615 *Geophys. Res.*, 90, 5710–5720, 1985.
- 616 Bauza, J. F., Morell, J. M., and Corredor, J. E.: Biogeochemistry of nitrous oxide production in
617 the red mangrove (*Rhizophora mangle*) forest sediments, *Estuar. Coast. Shelf Sci.*, 55, 697–
618 704, <https://doi.org/10.1006/ecss.2001.0913>, 2002.
- 619 Bridgham, S. D. and Richardson, C. J.: Mechanisms controlling soil respiration (CO₂ and CH₄)



- 620 in southern peatlands, *Soil Biol. Biochem.*, 24, 1089–1099, <https://doi.org/10.1016/0038->
621 0717(92)90058-6, 1992.
- 622 Brimblecombe, P.: The Global Sulfur Cycle, in: *Treatise on Geochemistry*, vol. 10, edited by:
623 Holland, H. D. and Turekian, K. K., Elsevier Science, 559–591,
624 <https://doi.org/10.1016/B978-0-08-095975-7.00814-7>, 2014.
- 625 Capone, D. G. and Kiene, R. P.: Comparison of microbial dynamics in marine and freshwater
626 sediment, *Limnol. Ocean.*, 33, 725–749, 1988.
- 627 Capooci, M. and Vargas, R.: Diel and seasonal patterns of soil CO₂ efflux in a temperate tidal
628 marsh, *Sci. Total Environ.*, 802, <https://doi.org/10.1016/j.scitotenv.2021.149715>, 2022.
- 629 Capooci, M., Barba, J., Seyfferth, A. L., and Vargas, R.: Experimental influence of storm-surge
630 salinity on soil greenhouse gas emissions from a tidal salt marsh, *Sci. Total Environ.*, 686,
631 1164–1172, <https://doi.org/10.1016/j.scitotenv.2019.06.032>, 2019.
- 632 Carroll, M. A., Heidt, L. E., Cicerone, R. J., and Prinn, R. G.: OCS, H₂S, and CS₂ fluxes from a
633 salt water marsh, *J. Atmos. Chem.*, 4, 375–395, <https://doi.org/10.1007/BF00053811>, 1986.
- 634 Cheng, X., Peng, R., Chen, J., Luo, Y., Zhang, Q., An, S., Chen, J., and Li, B.: CH₄ and N₂O
635 emissions from *Spartina alterniflora* and *Phragmites australis* in experimental mesocosms,
636 *Chemosphere*, 68, 420–427, <https://doi.org/10.1016/J.CHEMOSPHERE.2007.01.004>, 2007.
- 637 Cooper, D. J., De Mello, W. Z., Cooper, W. J., Zika, R. G., Saltzman, E. S., Prospero, J. M., and
638 Savoie, D. L.: Short-term variability in biogenic sulphur emissions from a Florida *Spartina*
639 *alterniflora* marsh, *Atmos. Environ.*, 21, 7–12, 1987a.
- 640 Cooper, W. J., Cooper, D. J., Saltzman, E. S., Mello, W. Z. d., Savoie, D. L., Zika, R. G., and
641 Prospero, J. M.: Emissions of biogenic sulphur compounds from several wetland soils in
642 Florida, *Atmos. Environ.*, 21, 1491–1495, [https://doi.org/10.1016/0004-6981\(87\)90311-8](https://doi.org/10.1016/0004-6981(87)90311-8),



- 643 1987b.
- 644 Dacey, J. W. H., King, G. M., and Wakeham, S. G.: Factors controlling emission of
645 dimethylsulphide from salt marshes, *Nature*, 330, 643–645,
646 <https://doi.org/10.1038/330643a0>, 1987.
- 647 DeLaune, R. D., Devai, I., and Lindau, C. W.: Flux of reduced sulfur gases along a salinity
648 gradient in Louisiana coastal marshes, *Estuar. Coast. Shelf Sci.*, 54, 1003–1011,
649 <https://doi.org/10.1006/ecss.2001.0871>, 2002.
- 650 Diefenderfer, H. L., Cullinan, V. I., Borde, A. B., Gunn, C. M., and Thom, R. M.: High-
651 frequency greenhouse gas flux measurement system detects winter storm surge effects on
652 salt marsh, *Glob. Chang. Biol.*, 24, 5961–5971, <https://doi.org/10.1111/gcb.14430>, 2018.
- 653 DNREC: Delaware National Estuarine Research Reserve Estuarine Profile, 158 pp., 1999.
- 654 Duarte, C. M., Middelburg, J. J., and Caraco, N.: Major role of marine vegetation on the oceanic
655 carbon cycle, 2, 1–8, <https://doi.org/10.1111/j.2042-7158.1975.tb10261.x>, 2005.
- 656 Emery, H. E. and Fulweiler, R. W.: *Spartina alterniflora* and invasive *Phragmites australis*
657 stands have similar greenhouse gas emissions in a New England marsh, *Aquat. Bot.*, 116,
658 83–92, <https://doi.org/10.1016/j.aquabot.2014.01.010>, 2014.
- 659 Emmer, I., Needelman, B., Emmett-Mattox, S., Crooks, S., Beers, L., Megonigal, P., Myers, D.,
660 Oreska, M., McGlathery, K., and Shoch, D.: Methodology for tidal wetland and seagrass
661 restoration, 1–115 pp., 2021.
- 662 Filippa, G., Cremonese, E., Migliavacca, M., Galvagno, M., Folker, M., Richardson, A. D., and
663 Tomelleri, E.: phenopix: process digital images of a vegetation cover, R Package. version
664 2.4.2, 2020.
- 665 Finster, K., King, G. M., Bak, F., and Finster, K.: Formation of methylmercaptan and



- 666 dimethylsulfide from methoxylated aromatic compounds in anoxic marine and fresh water
667 sediments, *FEMS Microbiol. Ecol.*, 74, 295–302, <https://doi.org/10.1111/j.1574->
668 [6968.1990.tb04076.x](https://doi.org/10.1111/j.1574-6968.1990.tb04076.x), 1990.
- 669 Goldan, P. D., Kuster, W. C., Albritton, D. L., and Fehsenfeld, F. C.: The measurement of
670 natural sulfur emissions from soils and vegetation: three sites in the Eastern United States
671 revisited, *J. Atmos. Chem.*, 5, 439–467, <https://doi.org/10.1007/BF00113905>, 1987.
- 672 Granville, K. E., Ooi, S. K., Koenig, L. E., Lawrence, B. A., Elphick, C. S., and Helton, A. M.:
673 Seasonal patterns of denitrification and N₂O production in a southern New England salt
674 marsh, 41, 1–13, <https://doi.org/10.1007/s13157-021-01393-x>, 2021.
- 675 Hill, A. C., Vázquez-Lule, A., and Vargas, R.: Linking vegetation spectral reflectance with
676 ecosystem carbon phenology in a temperate salt marsh, *Agric. For. Meteorol.*, 307, 108481,
677 <https://doi.org/10.1016/j.agrformet.2021.108481>, 2021.
- 678 Hines, M. E.: Emissions of sulfur gases from wetlands, 25, 153–161,
679 <https://doi.org/10.1080/05384680.1996.11904076>, 1996.
- 680 Järveoja, J., Nilsson, M. B., Gažovič, M., Crill, P. M., and Peichl, M.: Partitioning of the net CO₂
681 exchange using an automated chamber system reveals plant phenology as key control of
682 production and respiration fluxes in a boreal peatland, *Glob. Chang. Biol.*, 24, 3436–3451,
683 <https://doi.org/10.1111/gcb.14292>, 2018.
- 684 Jha, C. S., Rodda, S. R., Thumaty, K. C., Raha, A. K., and Dadhwal, V. K.: Eddy covariance
685 based methane flux in Sundarbans mangroves, India, *J. Earth Syst. Sci.*, 123, 1089–1096,
686 <https://doi.org/10.1007/s12040-014-0451-y>, 2014.
- 687 Jørgensen, B. B. and Okholm-Hansen, B.: Emissions of biogenic sulfur gases from a Danish
688 estuary, *Atmos. Environ.*, 19, 1737–1749, [https://doi.org/10.1016/0004-6981\(85\)90001-0](https://doi.org/10.1016/0004-6981(85)90001-0),



- 689 1985.
- 690 Kellogg, W. W., Cadle, R. D., Allen, E. R., Lazrus, A. L., and Martell, E. A.: The Sulfur Cycle,
691 Science., 4022 (175), 587–596, [https://doi.org/10.1016/S0074-6142\(08\)62696-0](https://doi.org/10.1016/S0074-6142(08)62696-0), 1972.
- 692 Kiene, R. P.: Dimethyl sulfide metabolism in salt marsh sediments, FEMS Microbiol. Lett., 53,
693 71–78, [https://doi.org/10.1016/0378-1097\(88\)90014-6](https://doi.org/10.1016/0378-1097(88)90014-6), 1988.
- 694 Kiene, R. P. and Visscher, P. T.: Production and fate of methylated sulfur compounds from
695 methionine and dimethylsulfoniopropionate in anoxic salt marsh Sediments, Appl. Environ.
696 Microbiol., 53, 2426–2434, 1987.
- 697 Kim, J., Verma, S. B., Billesbach, D. P., and Clement, R. J.: Diel variation in methane emission
698 from a midlatitude prairie wetland: significance of convective throughflow in *Phragmites*
699 *australis*, J. Geophys. Res. Atmos., 103, 28029–28039, <https://doi.org/10.1029/98JD02441>,
700 1998.
- 701 Koskinen, M., Minkkinen, K., Ojanen, P., Kämäräinen, M., Laurila, T., and Lohila, A.:
702 Measurements of CO₂ exchange with an automated chamber system throughout the year:
703 Challenges in measuring night-time respiration on porous peat soil, 11, 347–363,
704 <https://doi.org/10.5194/bg-11-347-2014>, 2014.
- 705 Laursen, A. E. and Seitzinger, S. P.: Measurement of denitrification in rivers: an integrated,
706 whole reach approach, Hydrobiologia, 485, 67–81, 2002.
- 707 Lin, Y. S., Heuer, V. B., Ferdelman, T. G., and Hinrichs, K.-U.: Microbial conversion of
708 inorganic carbon to dimethyl sulfide in anoxic lake sediment (Plußsee, Germany), 7, 2433–
709 2444, <https://doi.org/10.5194/bg-7-2433-2010>, 2010.
- 710 Livesley, S. J. and Andrusiak, S. M.: Temperate mangrove and salt marsh sediments are a small
711 methane and nitrous oxide source but important carbon store, Estuar. Coast. Shelf Sci., 97,



- 712 19–27, <https://doi.org/10.1016/j.ecss.2011.11.002>, 2012.
- 713 Lomans, B. P., Van der Drift, C., Pol, A., and Op den Camp, H. J. M.: Microbial cycling of
714 volatile organic sulfur compounds, *Water Sci. Technol.*, 45, 55–60,
715 <https://doi.org/10.1007/s00018-002-8450-6>, 2002.
- 716 Macreadie, P. I., Costa, M. D. P., Atwood, T. B., Friess, D. A., Kelleway, J. J., Kennedy, H.,
717 Lovelock, C. E., Serrano, O., and Duarte, C. M.: Blue carbon as a natural climate solution,
718 *Nat. Rev. Earth Environ.*, 2, 826–839, [https://doi.org/https://doi.org/10.1038/s43017-021-](https://doi.org/https://doi.org/10.1038/s43017-021-00224-1)
719 00224-1, 2021.
- 720 De Mello, W. Z., Cooper, D. J., Cooper, W. J., Saltzman, E. S., Zika, R. G., Savoie, D. L., and
721 Prospero, J. M.: Spatial and diel variability in the emissions of some biogenic sulfur
722 compounds from a Florida *Spartina alterniflora* coastal zone, *Atmos. Environ.*, 21, 987–990,
723 [https://doi.org/10.1016/0004-6981\(87\)90095-3](https://doi.org/10.1016/0004-6981(87)90095-3), 1987.
- 724 Middelburg, J. J., Klaver, G., Nieuwenhuize, J., Hass, W. De, Vlug, T., Nat, J. F. W. A. Van Der,
725 Middelburg, J. J., Klaver, G., Haas, W. De, Vlug, T., and Jaco, F.: Organic matter mineral
726 sediments along an estuarine gradient, *Mar. Ecol. Prog. Ser.*, 132, 157–168, 1996.
- 727 Möller, I., Kudella, M., Rupprecht, F., Spencer, T., Paul, M., Van Wesenbeeck, B. K., Wolters,
728 G., Jensen, K., Bouma, T. J., Miranda-Lange, M., and Schimmels, S.: Wave attenuation
729 over coastal salt marshes under storm surge conditions, *Nat. Geosci.*, 7, 727–731,
730 <https://doi.org/10.1038/NGEO2251>, 2014.
- 731 Moran, J. J., House, C. H., Vrentas, J. M., and Freeman, K. H.: Methyl sulfide production by a
732 novel carbon monoxide metabolism in *Methanosarcina acetivorans*, *Appl. Environ.*
733 *Microbiol.*, 74, 540–542, <https://doi.org/10.1128/AEM.01750-07>, 2008.
- 734 Morrison, M. C. and Hines, M. E.: The variability of biogenic sulfur flux from a temperate salt



- 735 marsh on short time and space scales, *Atmos. Environ. Part A. Gen. Top.*, 24A, 1771–1779,
736 [https://doi.org/10.1016/0960-1686\(90\)90509-L](https://doi.org/10.1016/0960-1686(90)90509-L), 1990.
- 737 Moseman-Valtierra, S., Gonzalez, R., Kroeger, K. D., Tang, J., Chao, W. C., Crusius, J., Bratton,
738 J., Green, A., and Shelton, J.: Short-term nitrogen additions can shift a coastal wetland from
739 a sink to a source of N₂O, *Atmos. Environ.*, 45, 4390–4397,
740 <https://doi.org/10.1016/j.atmosenv.2011.05.046>, 2011.
- 741 Moseman-Valtierra, S., Abdul-Aziz, O. I., Tang, J., Ishtiaq, K. S., Morkeski, K., Mora, J., Quinn,
742 R. K., Martin, R. M., Egan, K., Brannon, E. Q., Carey, J., and Kroeger, K. D.: Carbon
743 dioxide fluxes reflect plant zonation and belowground biomass in a coastal marsh, 7,
744 e01560, 2016.
- 745 Murray, R. H., Erler, D. V., and Eyre, B. D.: Nitrous oxide fluxes in estuarine environments:
746 response to global change, *Glob. Chang. Biol.*, 21, 3219–3245,
747 <https://doi.org/10.1111/gcb.12923>, 2015.
- 748 Van Der Nat, F. and Middelburg, J. J.: Methane emission from tidal freshwater marshes,
749 *Biogeochemistry*, 49, 103–121, 2000.
- 750 Neubauer, S. C. and Magonigal, J. P.: Correction to: Moving Beyond Global Warming Potentials
751 to Quantify the Climatic Role of Ecosystems, *Ecosyst. 2019* 228, 22, 1931–1932,
752 <https://doi.org/10.1007/S10021-019-00422-5>, 2019.
- 753 NOAA National Estuarine Research Reserve System (NERRS): System-wide monitoring
754 program, 2015
- 755 Oremland, R. S., Marsh, L. M., and Polcin, S.: Methane production and simultaneous sulphate
756 reduction in anoxic, salt marsh sediments, *Nature*, 296, 143–145, 1982.
- 757 Peterson, P. M., Romaschenko, K., Arrieta, Y. H., and Saarela, J. M.: A molecular phylogeny



- 758 and new subgeneric classification of *Sporobolus* (Poaceae: Chloridoideae: Sporobolinae),
759 *Taxon*, 63, 1212–1243, <https://doi.org/10.12705/636.19>, 2014.
- 760 Petrakis, S., Seyfferth, A., Kan, J., Inamdar, S., and Vargas, R.: Influence of experimental
761 extreme water pulses on greenhouse gas emissions from soils, *Biogeochemistry*, 133,
762 147–164, <https://doi.org/10.1007/s10533-017-0320-2>, 2017.
- 763 Rinne, J., Riutta, T., Pihlatie, M., Aurela, M., Haapanala, S., Tuovinen, J. P., Tuittila, E. S., and
764 Vesala, T.: Annual cycle of methane emission from a boreal fen measured by the eddy
765 covariance technique, *Tellus, Ser. B Chem. Phys. Meteorol.*, 59, 449–457,
766 <https://doi.org/10.1111/j.1600-0889.2007.00261.x>, 2007.
- 767 Rosentreter, J. A., Maher, D. T., Erler, D. V., Murray, R. H., and Eyre, B. D.: Methane emissions
768 partially offset “blue carbon” burial in mangroves, *Sci. Adv.*, 4, eaao4985,
769 <https://doi.org/10.1126/SCIADV.AAO4985>, 2018.
- 770 Rosentreter, J. A., Al-Haj, A. N., Fulweiler, R. W., and Williamson, P.: Methane and nitrous
771 oxide emissions complicate coastal blue carbon assessments, *Global Biogeochem.*
772 *Cycles*, 35, e2020GB006858, <https://doi.org/10.1029/2020GB006858>, 2021.
- 773 Savage, K., Phillips, R., and Davidson, E.: High temporal frequency measurements of
774 greenhouse gas emissions from soils, 11, 2709–2720, [https://doi.org/10.5194/bg-11-](https://doi.org/10.5194/bg-11-2709-2014)
775 [2709-2014](https://doi.org/10.5194/bg-11-2709-2014), 2014.
- 776 Sela-Adler, M., Said-Ahmad, W., Sivan, O., Eckert, W., Kiene, R. P., and Amrani, A.: Isotopic
777 evidence for the origin of dimethylsulfide and dimethylsulfoniopropionate-like
778 compounds in a warm, monomictic freshwater lake, *Environ. Chem.*, 13, 340–351,
779 <https://doi.org/https://doi.org/10.1071/EN15042>, 2015.
- 780 Seyednasrollah, B., Young, A. M., Hufkens, K., Milliman, T., Friedl, M. A., Frohling, S.,



- 781 Richardson, A. D., Abraha, M., Allen, D. W., Apple, M., Arain, M. A., Baker, J., Baker,
782 J. M., Baldocchi, D., Bernacchi, C. J., Bhattacharjee, J., Blanken, P., Bosch, D. D.,
783 Boughton, R., Boughton, E. H., [...] Zona, D.: PhenoCam dataset v2.0: Vegetation
784 phenology from digital camera imagery, Oak Ridge, Tennessee,
785 <https://doi.org/https://doi.org/10.3334/ORNLDAAC/1674>, 2019.
- 786 Seyfferth, A. L., Bothfeld, F., Vargas, R., Stuckey, J. W., Wang, J., Kearns, K., Michael, H. A.,
787 Guimond, J., Yu, X., and Sparks, D. L.: Spatial and temporal heterogeneity of
788 geochemical controls on carbon cycling in a tidal salt marsh, *Geochim. Cosmochim.*
789 *Acta*, 282, 1–18, <https://doi.org/10.1016/j.gca.2020.05.013>, 2020.
- 790 Simpson, L. T., Osborne, T. Z., and Feller, I. C.: Wetland soil CO₂ efflux along a latitudinal
791 gradient of spatial and temporal complexity, 42, 45–54, [https://doi.org/10.1007/s12237-](https://doi.org/10.1007/s12237-018-0442-3)
792 018-0442-3, 2019.
- 793 Steudler, P. A. and Peterson, B. J.: Contribution of gaseous sulphur from salt marshes to the
794 global sulphur cycle, *Nature*, 311, 455–457, <https://doi.org/10.1038/311455a0>, 1984.
- 795 Steudler, P. A. and Peterson, B. J.: Annual cycle of gaseous sulfur emissions from a New
796 England *Spartina alterniflora* marsh, *Atmos. Environ.*, 19, 1411–1416,
797 [https://doi.org/10.1016/0004-6981\(85\)90278-1](https://doi.org/10.1016/0004-6981(85)90278-1), 1985.
- 798 Taubman, S. J. and Kasting, J. F.: Carbonyl sulfide: no remedy for global warming, *Geophys.*
799 *Res. Lett.*, 22, 803–805, <https://doi.org/10.1029/95GL00636>, 1995.
- 800 Tong, C., Huang, J. F., Hu, Z. Q., and Jin, Y. F.: Diurnal variations of carbon dioxide, methane,
801 and nitrous oxide vertical fluxes in a subtropical estuarine marsh on neap and spring tide
802 days, 36, 633–642, <https://doi.org/10.1007/s12237-013-9596-1>, 2013.
- 803 Tong, C., Morris, J. T., Huang, J., Xu, H., and Wan, S.: Changes in pore-water chemistry and



- 804 methane emission following the invasion of *Spartina alterniflora* into an oligohaline
805 marsh, *Limnol. Oceanogr.*, 63, 384–396, <https://doi.org/10.1002/lno.10637>, 2018.
- 806 Trifunovic, B., Vázquez-Lule, A., Capooci, M., Seyfferth, A. L., Moffat, C., and Vargas, R.:
807 Carbon dioxide and methane emissions from temperate salt marsh tidal creek, J.
808 *Geophys. Res. Biogeosciences*, 125, <https://doi.org/10.1029/2019JG005558>, 2020.
- 809 UNFCCC: Paris Agreement, 2015.
- 810 Vargas, R., Carbone, M. S., Reichstein, M., and Baldocchi, D. D.: Frontiers and challenges in
811 soil respiration research: from measurements to model-data integration, *Biogeochemistry*,
812 102, 1–13, <https://doi.org/10.1007/s10533-010-9462-1>, 2011.
- 813 Vázquez-Lule, A. and Vargas, R.: Biophysical drivers of net ecosystem and methane exchange
814 across phenological phases in a tidal salt marsh, *Agric. For. Meteorol.*, 300,
815 <https://doi.org/10.1016/j.agrformet.2020.108309>, 2021.
- 816 Wang, J. and Wang, J.: *Spartina alterniflora* alters ecosystem DMS and CH₄ emissions and their
817 relationship along interacting tidal and vegetation gradients within a coastal salt marsh in
818 Eastern China, *Atmos. Environ.*, 167, 346–359,
819 <https://doi.org/10.1016/J.ATMOSENV.2017.08.041>, 2017.
- 820 Ward, N., Magonigal, P. J., Bond-Lamberty, B., Bailey, V., Butman, D., Canuel, E.,
821 Diefenderfer, H., Ganju, N. K., Goñi, M. A., Graham, E. B., Hopkinson, C. S.,
822 Khangaonkar, T., Langley, J. A., McDowell, N. G., Myers-Pigg, A. N., Neumann, R. B.,
823 Osburn, C. L., Price, R. M., Rowland, J., Sengupta, A., Simard, M., Thornton, P. E.,
824 Tzortziou, M., Vargas, R., Weisenhorn, P. B., and Windham-Myers, L.: Representing the
825 function and sensitivity of coastal interfaces in earth system models, *Nat. Commun.*, 11,
826 1–14, <https://doi.org/10.1038/s41467-020-16236-2>, 2020.



- 827 Watts, S. F.: The mass budgets of carbonyl sulfide, dimethyl sulfide, carbon disulfide and
828 hydrogen sulfide, *Atmos. Environ.*, 34, 761–779, <https://doi.org/10.1016/S1352->
829 2310(99)00342-8, 2000.
- 830 Whelan, M. E., Min, D. H., and Rhew, R. C.: Salt marsh vegetation as a carbonyl sulfide (COS)
831 source to the atmosphere, *Atmos. Environ.*, 73, 131–137,
832 <https://doi.org/10.1016/J.ATMOSENV.2013.02.048>, 2013.
- 833 Wilson, B. J., Mortazavi, B., and Kiene, R. P.: Spatial and temporal variability in carbon dioxide
834 and methane exchange at three coastal marshes along a salinity gradient in a northern
835 Gulf of Mexico estuary, *Biogeochemistry*, 123, 329–347, <https://doi.org/10.1007/s10533->
836 015-0085-4, 2015.
- 837 Xie, H. and Moore, R. M.: Carbon disulfide in the North Atlantic and Pacific Oceans, *J.*
838 *Geophys. Res. Ocean.*, 104, 5393–5402, <https://doi.org/10.1029/1998jc900074>, 1999.
- 839 Xie, X., Zhang, M.-Q., Zhao, B., and Guo, H.-Q.: Dependence of coastal wetland ecosystem
840 respiration on temperature and tides: a temporal perspective, 11, 539–545,
841 <https://doi.org/10.5194/bg-11-539-2014>, 2014.
- 842 Xu, X., Fu, G., Zou, X., Ge, C., and Zhao, Y.: Diurnal variations of carbon dioxide, methane,
843 and nitrous oxide fluxes from invasive *Spartina alterniflora* dominated coastal wetland in
844 northern Jiangsu Province, *Acta Oceanol. Sin.*, 36, 105–113,
845 <https://doi.org/10.1007/s13131-017-1015-1>, 2017.
- 846 Yang, W.-B., Yuan, C.-S., Huang, B.-Q., Tong, C., and Yang, L.: Emission characteristics of
847 greenhouse gases and their correlation with water quality at an estuarine mangrove
848 ecosystem – the application of an in-situ on-site NDIR monitoring technique, *Wetl.* 2018
849 384, 38, 723–738, <https://doi.org/10.1007/S13157-018-1015-8>, 2018.



850 Yang, W.-B. Bin, Yuan, C.-S. S., Tong, C., Yang, P., Yang, L., and Huang, B.-Q. Q.: Diurnal
851 variation of CO₂, CH₄, and N₂O emission fluxes continuously monitored in-situ in three
852 environmental habitats in a subtropical estuarine wetland, *Mar. Pollut. Bull.*, 119, 289–
853 298, <https://doi.org/10.1016/j.marpolbul.2017.04.005>, 2017.

854 Yu, X., Ye, S., Olsson, L., Wei, M., Krauss, K. W., and Brix, H.: A 3-year in-situ measurement
855 of CO₂ efflux in coastal wetlands: understanding carbon loss through ecosystem
856 respiration and its partitioning, <https://doi.org/10.1007/s13157-019-01197-0>, 2019.

857 Yu, Z., Li, Y., Deng, H., Wang, D., Chen, Z., and Xu, S.: Effect of *Scirpus mariqueter* on nitrous
858 oxide emissions from a subtropical monsoon estuarine wetland, *J. Geophys. Res.*
859 *Biogeosciences*, 117, 2017, <https://doi.org/10.1029/2011JG001850>, 2012.

860 Zhang, Y., Wang, L., Xie, X., Huang, L., and Wu, Y.: Effects of invasion of *Spartina*
861 *alterniflora* and exogenous N deposition on N₂O emissions in a coastal salt marsh, *Ecol.*
862 *Eng.*, 58, 77–83, <https://doi.org/10.1016/j.ecoleng.2013.06.011>, 2013.

863